



# Modular micropumps fabricated by 3D printed technologies for polymeric microfluidic device applications

Y. Alvarez-Braña<sup>a,b,1</sup>, J. Etxebarria-Elezgarai<sup>a,1,2</sup>, L. Ruiz de Larrinaga-Vicente<sup>a,b</sup>, F. Benito-Lopez<sup>b,c,d,\*</sup>, L. Basabe-Desmonts<sup>a,c,d,e,\*</sup>

<sup>a</sup> Microfluidics Cluster UPV/EHU, BIOMICS microfluidics Group, Lascaray Research Center, University of the Basque Country UPV/EHU, Vitoria-Gasteiz, Spain

<sup>b</sup> Microfluidics Cluster UPV/EHU, Analytical Microsystems & Materials for Lab-on-a-Chip (AMMa-LOAC) Group, Analytical Chemistry Department, University of the Basque Country UPV/EHU, Spain

<sup>c</sup> Bioaraba Health Research Institute, Microfluidics Cluster UPV/EHU, Vitoria-Gasteiz, Spain

<sup>d</sup> BCMaterials, Basque Center for Materials, Applications and Nanostructures, UPV/EHU Science Park, Leioa, Spain

<sup>e</sup> Basque Foundation of Science, IKERBASQUE, María Díaz Haroko Kalea, 3, Bilbao, 48013, Spain

## ARTICLE INFO

### Keywords:

Self-powered microfluidics  
Micropumps  
Degas driven flow  
3D printing  
Stereolithography  
Starch-lugol reaction

## ABSTRACT

In order to facilitate the implementation of microfluidic technology for rapid point-of-care analysis, there is a demand for self-powered microfluidics. The modular architecture of degas driven plug-and-play polymeric micropumps and microfluidic cartridges arose during last decade as a powerful strategy for autonomous flow control. So far, reported polymeric micropumps were made of poly-dimethyl siloxane and were fabricated by casting. In this work, we showed that the advantages of three-dimensional printing can greatly benefit the development of modular micropumps. In addition, micropumps were created with a geometry that cannot be manufactured with conventional techniques, making it easily assemblable to microfluidic devices. Four types of polymeric resins and three printing methods were used to create a set of functional micropumps. It was shown that the material and the design of the printed micropumps were related to their power, making them tuneable and programmable. Finally, as proof of concept, a self-powered colorimetric test for the detection of starch was demonstrated. Three-dimensional printed micropumps emerge as an innovative element in the field of self-powered microfluidics, which may be the key to develop integrated microsystems for several applications such as in rapid point-of-care analysis.

## 1. Introduction

Most miniaturised analytical devices need rigorous fluidic control, which require external power sources connected to the microfluidic cartridge. In contrast, self-powered microfluidic devices provide new ways of fluidic control without the need of external electronic components or moving parts. Methods like finger actuated pumps [1], effervescent pumps [2], capillary driven flows [3], paper driven flows [4] (including paper lateral flows and paper microfluidics components), threat-based devices [5,6] and, in particular, stimuli responsive materials [7–9] are being integrated within microfluidic devices for fluid manipulation and flow control at the microscale. Additionally, many publications are demonstrating the effectiveness of the “degas driven

flow” technique using polydimethylsiloxane (PDMS). PDMS is a highly porous and air permeable material composed of flexible silicon-oxygen chains that provide free volumes within its structure, allowing gas diffusion [10]. Therefore, it is commonly used in the fabrication of microfluidic systems. To trigger the “degas driven flow” process, the PDMS is activated by extracting the air contained within its structure. Then, once the degassed material is subjected to atmospheric pressure, it absorbs air from the microfluidic channel (and from its surroundings as well) to balance its internal pressure. Consequently, a negative pressure is generated inside the microfluidic channel, which leads to suction forces capable of generating fluidic motion. The dynamics of the PDMS degas driven flow depend on the channel and device geometries and are sensitive to several parameters as described by Zhao et al. [11] and

\* Corresponding authors at: Microfluidics Cluster UPV/EHU, University of the Basque Country, Vitoria-Gasteiz, Spain.

E-mail addresses: [fernando.benito@ehu.es](mailto:fernando.benito@ehu.es) (F. Benito-Lopez), [lourdes.basabe@ehu.es](mailto:lourdes.basabe@ehu.es) (L. Basabe-Desmonts).

<sup>1</sup> Both authors contribute equally to this work.

<sup>2</sup> Current address at: CIC nanoGUNE BRTA, Tolosa Hiribidea 76, 20018 Donostia - San Sebastián, Spain.

Liang et al. [12]. Several applications, such as Point-of-Care (POC) diagnostics [13,14]; digital PCR [15]; or DNA analysis [16,17], have been demonstrated based on this mechanism for flow control. With the idea of having modular universal architectures for self-powered microfluidics, several reports demonstrated the possibility of manufacturing modular polymeric plug-and-play micropumps based on the concept of degas driven flow [11,18]. These PDMS micropumps were fabricated to drive flows inside microchannels of polymer microfluidic devices (e.g. cyclo olefin polymer, poly(methyl methacrylate), pressure sensitive adhesive, etc). The flow generated by these PDMS micropumps could be tuned by just changing the effective surface area to volume ratio of the micropump or the permeability degree of the PDMS, allowing the control of the flow inside the microchannels [18]. However, those modular micropumps are manufactured by casting methods using moulds, a slow and low throughput technique. The idea of a universal modular system holds great promise for the improvement of generic architectures for POC analysis devices, but, in order to get to that point, it is necessary to have a versatile manufacturing technique that would enable the easy fabrication of customised micropumps and cartridge designs. Three-dimensional (3D) printing technology constitutes a manufacturing revolution, which is being incorporated in industrial processes, research activities and education. It provides the means for rapid fabrication of prototypes and end-use products, enabling mass customisation and manufacturing of pieces with complex geometric shapes [19]. It is well accepted that additive approaches will allow the creation of hybrid multifunctional pieces by non-assembly processes [20]. As expected, this technology is impacting the microfluidics community, as reviewed by Au [21], Gross [22], Arivarasi [23] and Mi [24], where numerous examples are reported on the 3D printing fabrication of microfluidic devices [25–28] and components [29,30] by different methodologies, such as additive printing and stereolithography (SLA), with the number of publications exponentially increasing in the last few years. Recent advances (e.g., increased accuracy and reduced printing times) are allowing to print microfluidic devices and components with geometries that could not be fabricated by traditional machinery or moulding methods [31]. Other actuators, like valves or multi-component pumps that were previously manufactured by casting and moulding of PDMS, are nowadays manufactured using techniques, such as SLA; fused deposition modelling (FDM); multijet modelling fabrication (MJM); digital light processing (DLP), etc. [32], in order to obtain more cost-effective devices. Recently, significant progresses have been made in the development of 3D printed devices thanks to the use of novel flexible and easily printable materials, enabling the replacement

of PDMS [33], the manufacture of external peristaltic pumps [34,35] or tesla pumps [36] and the fabrication, fully or partially, of integrated micropumps, which are non-degas-actuated but based on moving parts, into microfluidic devices [37–42].

Inspired by our previous work on PDMS micropumps and the progress on 3D printing technologies, we have evaluated how 3D printing would enable fast prototyping and fabrication of modular plug-and-play polymeric micropumps using different materials, fabrication techniques and geometries (Fig. 1). Herein we present the fabrication of self-powered modular micropumps by three different 3D-printing techniques (SLA, DLP and FDM) and the characterisation of their performance when integrated into portable and low cost microfluidic cartridges fabricated in diverse polymeric materials (PMMA, PDMS, polymeric resin, ...). As a proof of concept, we used a 3D printed micropump assembled to a polymeric microfluidic cartridge as a self-powered microfluidic device for the colorimetric starch detection.

## 2. Materials and methods

### 2.1. 3Dp- $\mu$ Pumps fabrication

3Dp- $\mu$ Pumps were fabricated by different 3D printing techniques: (1) stereolithography of two flexible resins; (2) digital light processing of a blue resin; and (3) fused deposition modelling of a thermoplastic filament.

#### 2.1.1. By stereolithography

The SLA 3Dp- $\mu$ Pumps were fabricated as a single piece unit, by means of a stereolithography 3D printer (Form 1 + SLA 3D Printer, Formlabs) with two flexible photopolymer resins, FLFLGR02 (black) and FLFLGR01 (clear) (Formlabs, U.S.A.) using 100  $\mu$ m and 50  $\mu$ m printing resolution, respectively. Creo Parametrics 2.0 CAD software was used to design the 3D models and PreForm software was employed to build the supports and the foundation for the parts, in order to obtain a good printing. All support configurations were designed to produce a flat surface in the sealing zone of the 3Dp- $\mu$ Pump and thus, assure satisfactory bonding between the different pump units. After printing, the pumps were rinsed in an ultrasonic assisted isopropanol (Scharlab, Spain) bath for 15 min and post-cured under UV at 365 nm for 30 min (light source: LED lamp, MKM012405WH1, 25 W, ADEO). The supports were removed using a snip.

To fabricate multiple-unit pumps, two different 3Dp- $\mu$ Pump units were fabricated and assembled. On one hand, the top/individual

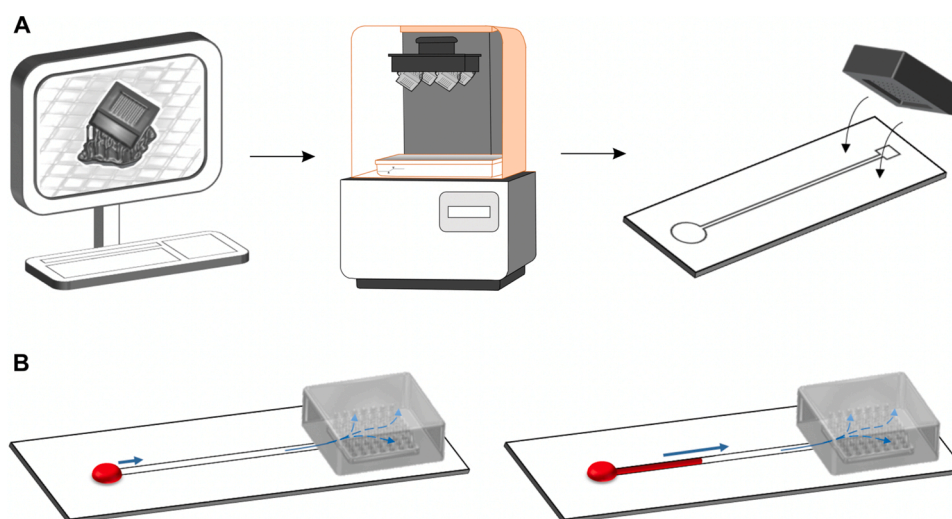


**Fig. 1.** Scheme of the 3Dp- $\mu$ Pumps actuation principle. (A) The 3D printed 3Dp- $\mu$ Pumps were vacuum pressurised and placed on the outlet of a microfluidic device. (B) The 3Dp- $\mu$ Pumps absorb the air inside the microchannels, creating a negative pressure and producing a suction force.

micropump unit has an upper resin cover that seals the internal cavities from the exterior and, on the other hand, an intermediate unit whose cylindrical cavities perforate the entire structure, Fig. SI-1. The dimensions of the two structures were: (1) top/individual unit:  $23 \times 23 \times 8 \text{ mm}^3$ ; (2) intermediate unit:  $23 \times 23 \times 7 \text{ mm}^3$ . These two configurations were stacked to each other through a transparent, double side pressure sensitive adhesive (PSA) layer (Adhesive Research, Ireland), sealing the different micropump units to each other. All intermediary units were internally connected through cylindrical cavities ( $800 \mu\text{m}$  diameter) to enable the air connection between the chambers of the different units. The pumps were connected to the microfluidic device using a PSA piece as well.

### 2.1.2. By digital light processing

The DLP 3Dp- $\mu$ Pumps were fabricated as a single piece, using the same design as for the SLA individual unit, by means of a digital light processing 3D printer (Kelant S400, Shenzhen Kelant Technology Co. Ltd, China) using  $100 \mu\text{m}$  printing resolution and a blue photopolymer resin (3D RAPID Blue, Monocure 3D, Australia). After printing, the 3Dp- $\mu$ Pumps were cleaned and the supports were removed using a snip. The flexibility of the resulting pieces was found to be lower than the SLA 3Dp- $\mu$ Pumps because of the composition of the resin. The pumps were connected to the microfluidic device using a PSA piece.

### 2.1.3. By fused deposition modelling

The FDM 3Dp- $\mu$ Pump was designed and fabricated at Optimus 3D S. L., Vitoria-Gasteiz, Spain. The pumps were printed as a single piece using a fused deposition 3D printer (Dynamical Tools DT600, Dynamical 3D, Spain) and a flexible thermoplastic filament (Thermoplastic Polyurethane, Blue TPU, Dynamical 3D, Spain). The final 3Dp- $\mu$ Pump has a cylindrical body ( $30 \text{ mm}$  diameter  $\times$   $17 \text{ mm}$  height) and a conical bottom ( $5 \text{ mm}$  height  $\times$   $30 \text{ mm}$  upper diameter  $\times$   $16 \text{ mm}$  lower diameter) with a circular perforation ( $12 \text{ mm}$  diameter) for direct connection to the chip without the use of a PSA piece. In order to increase the total surface area exposed to the microchannel, the internal structure of the pump was emptied with the exception of the cylindrical area, in which a mesh-like (90 % of infill) interlacing of filaments was made, a type of structure impossible to reproduce using any moulding technique, see Fig. SI-2.

## 2.2. 3Dp- $\mu$ Pumps degassing

3Dp- $\mu$ Pumps were degassed under vacuum (RVR003H-01 Vacuum Chamber, Dekker Vacuum Technologies, USA), for 2 h at 0.7 mbar, and vacuum-packed (SV-204 Vacuum Sealer, Sammic, Spain) in order to store them in airless environment, ready for use (Fig. SI-3).

## 2.3. Microfluidic chip fabrication

Microfluidics devices were fabricated by different methods: (1) multilayer lamination of PMMA, COP and PSA sheets; (2) 3D printing of open channels and subsequent assembly to a PSA layer; and (3) soft lithography by PDMS replication of SU8 moulds.

### 2.3.1. Multilayer laminated PMMA devices

PMMA sheets of different thicknesses ( $175 \mu\text{m}$  or  $380 \mu\text{m}$ ) layers were cut by a  $\text{CO}_2$  Laser System (VLS2.30 Desktop Universal Laser System) equipped with a  $10.6 \mu\text{m}$   $\text{CO}_2$  laser source ranging in power from 10 to 30 W. The layers of  $380 \mu\text{m}$  (ME303001, clear, Goodfellow) thickness were used to generate the microfluidic channel and the layers of  $175 \mu\text{m}$  (ME303016, clear, Goodfellow) thickness for the bottom and cover layers. The PMMA layers were assembled together and sealed by thermocompression bonding in a roller laminator (Vivid Matrix Duo Laminator MD-460/MD-650, Matrix) at  $105 \text{ }^\circ\text{C}$  to build the microfluidic chip. The microchannel dimensions were  $1 \text{ mm}$  wide,  $55 \text{ mm}$  long and  $380 \mu\text{m}$  height.

For the fabrication of the starch detection device a  $1.1 \text{ mm}$  thick

PMMA substrate (ME303010, clear, Goodfellow), grafted by the  $\text{CO}_2$  Laser System was used as the bottom of the device. This PMMA layer included a trench to deposit the sample, containing the gelled starch inside the channel. Microfluidic channels were cut by Graphtec Cutting Plotter CE6000–40 (CPS Cutter Printer Systems, Spain) on substrates of white PSA layers ( $127 \mu\text{m}$  thick ARcare® 8939). The top layer used to close the device was also cut by the same Graphtec Cutting Plotter on a substrate of COP ( $188 \mu\text{m}$  mcs–COP-02, Microfluidic ChipShop). After the lamination, a transparent PSA ( $50 \mu\text{m}$  thick ARcare® 92712) layer was used to seal the bottom of the device and  $10 \mu\text{L}$  of the starch gel was placed in the trench from a starch solution (Starch, extra pure, Fisher Scientific, Spain) in water,  $300 \text{ mM}$ , boiled at  $100 \text{ }^\circ\text{C}$  to promote gelation. Finally, the same transparent PSA layer was used to seal the trench after the sample addition and to connect a PMMA reservoir to the inlet of the device. To test the colorimetric reaction, a solution of potassium iodide with iodine in water (Lugols Iodine, Fisher Scientific, Spain) was pipetted in the inlet of the microfluidic device after the 3Dp- $\mu$ Pump assembly.

### 2.3.2. 3D printed devices

The 3D printed devices were designed and fabricated at Optimus 3D S.L., using Polyjet technology (Objet30 Pro, Stratasys Ltd., U.S.A.), a  $28 \mu\text{m}$  Z-axis printing resolution and an optically clear acrylic material (VeroClear, Stratasys Ltd., U.S.A.). The parts were designed using Objet Studio software. The final device was composed of a circular inlet ( $5 \text{ mm}$  diameter); a channel of  $100 \mu\text{m}$  height,  $1 \text{ mm}$  width and  $50 \text{ mm}$  length; and a circular outlet ( $10 \text{ mm}$  diameter) with walls in order to connect the FDM pump without any adhesive material. A pressure sensitive adhesive substrate (white PSA layers  $127 \mu\text{m}$  thick ARcare® 8939) was used as a bottom layer of the device. With the use of this design, another PSA layer to connect the micropump is not needed, therefore, this configuration allows an easier and faster connection method between the micropump and the microfluidic devices.

### 2.3.3. PDMS device

PDMS microfluidic devices were fabricated by soft lithography using a SU8 mould, as described in previous works in our group [43]. Briefly, a Mylar® photomask was designed and produced for the manufacture of the SU-8 master on silicon wafers. After the fabrication of the PDMS devices at a 10:1 ratio, they were cut and perforated with a  $2 \text{ mm}$  diameter puncher to create the inlet and outlet. Finally, the PDMS devices and a glass microscope slide were treated under air plasma for  $5 \text{ min}$  and assembled together to form the microfluidic chip. The specific dimensions of the channel were  $30 \mu\text{m}$  high,  $100 \mu\text{m}$  wide and  $50 \text{ cm}$  long.

## 2.4. 3Dp- $\mu$ Pumps – microchip assembly

In order to test the performance of the pumps, degassed SLA (FLFLGL01 and FLFLGL02) and DLP 3Dp- $\mu$ Pumps were assembled to the different devices using a PSA piece ( $50$  or  $147 \mu\text{m}$  thick ARcare® 92712 or 90880, depending on availability). The FDM 3Dp- $\mu$ Pumps were directly connected to the 3D printed chip without the use of any PSA layer.

## 2.5. Characterisation of 3Dp- $\mu$ Pumps flow rates

In general, the movement of the liquid inside the microchannels was recorded using a photographic camera (SONY Cyber-Shot DSC-RX100). From this data, the generated average flow rate values were estimated considering the microchannel cross section.

For the characterisation of the flow rate changes over time and the evaluation of the multiple-units of SLA-black 3Dp- $\mu$ Pumps (FLFLGR02), the micropumps were assembled on PMMA microfluidic chips ( $380 \mu\text{m}$  height,  $1 \text{ mm}$  width and  $50 \text{ mm}$  length). A reservoir (Female Luer Lok compatible connector with wide base, PMMA, ChipShop, Germany) for

sample loading was adhered to the inlet of the microfluidic chip. The 3Dp- $\mu$ Pumps and the reservoir were sealed using PSA piece (50  $\mu$ m thick ARcare® 92712). The set-up used for the characterisation consisted of a digital microscope (Mighty Scope 1.3 M Digital Microscope, Aven) to monitor the liquid front motion inside the microchannel by means of a gauge ruler placed on top of the microchannel, Fig. SI-4.

### 3. Results and discussion

#### 3.1. Modular 3Dp- $\mu$ Pumps, fabrication and performance

The mayor advantages of producing customizable modular micropumps by 3D printing technologies are: (1) the high amount of materials and printing technologies available, generating a large variety of micropumps compositions with different suction properties; and (2) it enables the direct fabrication of micropumps with optimal shapes and structures, which are not possible to manufacture with classical fabrication techniques such as milling, moulding or embossing. In order to demonstrate this versatility, micropumps were fabricated using diverse materials and techniques. Four polymeric resins were used, two flexible photopolymer resins (FLFLGR01 and FLFLGR02), a rigid photopolymeric resin (3D Rapid Blue) and a thermoplastic filament (blue TPU). And three 3D printing techniques were applied: two light directed fabrication techniques, SLA and DLP, and an additive printing technique, FDM.

Among this 3D printing methods, additive techniques (such as FDM) are faster than light directed printing, less expensive and highly extended nowadays. FDM consists on the heating and striding of a thermoplastic filament to be deposited on a surface layer by layer, creating a 3D model.

The fabrication of four micropumps with different designs was evaluated. The design of the pumps manufactured by SLA and DLP contained cylindrical cavities of 800  $\mu$ m in diameter and 4 mm in depth. The function of these cavities was to increase the air suction surface of the micropump, and, therefore, its power to move liquids through the microchannels. On the other hand, the FDM printed pump had a filament filling density of 90 %, to facilitate the suction of air by the material. The four micropumps were successfully printed. Pictures of each of them can be seen in Fig. 2.

In order to demonstrate that these modular 3Dp- $\mu$ Pumps could be used with a variety of microfluidic devices, microfluidic cartridges of different materials and dimensions were fabricated. In particular, three cartridges were fabricated: (1) a multilayer thermolaminated PMMA

device with a microchannel of 380  $\mu$ m height, 1 mm width and 50 mm length dimensions; (2) a 3D printed device with a 100  $\mu$ m height, 1 mm width and 40 mm length microchannel; and (3) a PDMS device containing a 30  $\mu$ m height, 10  $\mu$ m width and 50 cm length serpentine, a much smaller microchannel than the previous ones, Fig. 3. Then, a SLA-clear 3Dp- $\mu$ Pump was attached to the PMMA device, a FDM 3Dp- $\mu$ Pump was connected to the 3D printed device and a SLA-black 3Dp- $\mu$ Pump was connected to the PDMS serpentine device. For their evaluation, these degassed 3Dp- $\mu$ Pumps were mounted at the outlet of the device. To create an air leak-free closure of the system the SLA micropumps were bonded with a double side adhesive layer (see methods section), while the FDM micropump could be assembled directly with the chip, thanks to its unique design (Fig. 3D). Then, 90  $\mu$ L of red dyed water were added to the inlet of the microchannels and the movement of the liquid inside the channel was observed. In all the cases the negative pressure performed by the micropumps was enough to trigger the flow of liquid inside the microchannels, even in the smaller ones made of PDMS, which was the device with the greatest fluidic resistance (see Fig. 3 and Videos 1, 2 and 3). These results demonstrated the ability of the 3Dp- $\mu$ Pumps to generate continuous flows inside a variety of microfluidic cartridges. Even though the FDM printing technique has a lower precision than the light directed printing techniques, the use of additive printing provided with a highly extended and low-cost fabrication technique that allowed, as well, the generation of controllable degas-driven flows.

A key parameter that determines the pressure generated by the micropumps in the microchannels and, therefore, the flow rate of the fluids, is the permeability of the material of the micropump to air [18]. Hence, it was expected that different materials with different properties gave rise to micropumps that can move liquids at different speeds within the same fluidic structure. We evaluated the performance of the SLA-black, SLA-clear and DLP micropumps, which had the same design but were composed of different materials. SLA-black, SLA-clear and DLP micropumps were attached to a multilayer PMMA thermolaminated device (380  $\mu$ m height, 1 mm width and 50 mm length). Then, 90  $\mu$ L of red dyed water were added to the inlet of the microchannels and the movement of the liquid inside the channel was monitored. It was observed that the flow rates obtained using SLA-black, SLA-clear or DLP micropumps were  $0.30 \pm 5 \%$ ,  $0.50 \pm 8 \%$  and  $4.10 \pm 15 \%$   $\mu$ L  $\text{min}^{-1}$ , respectively (see Fig. 4 and Videos 4, 1 and 5). These diverse flow rates were expected since the chemical composition of each resin was different and their air solubility and air absorption properties were expected to differ from each other.

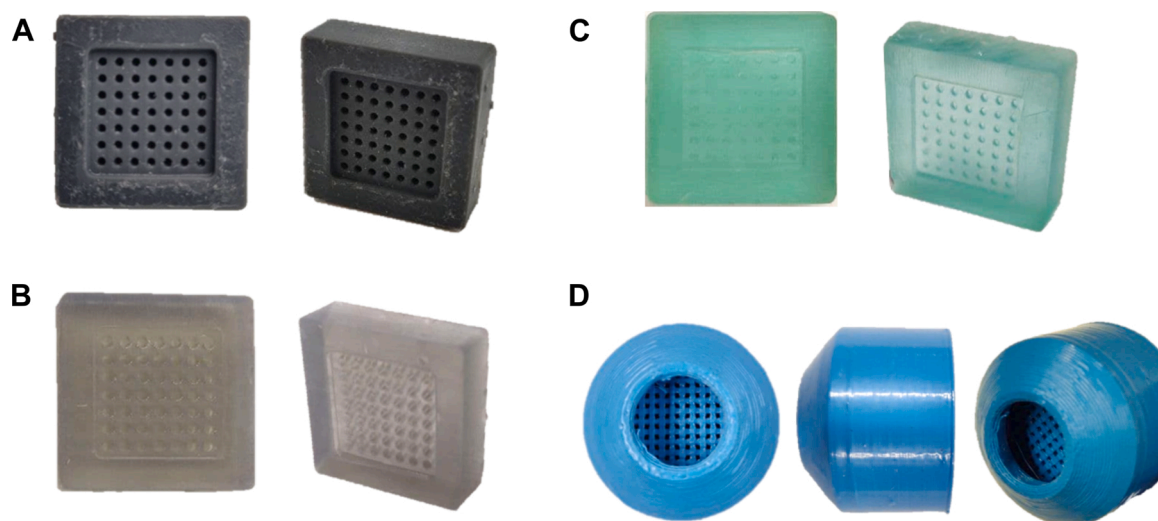
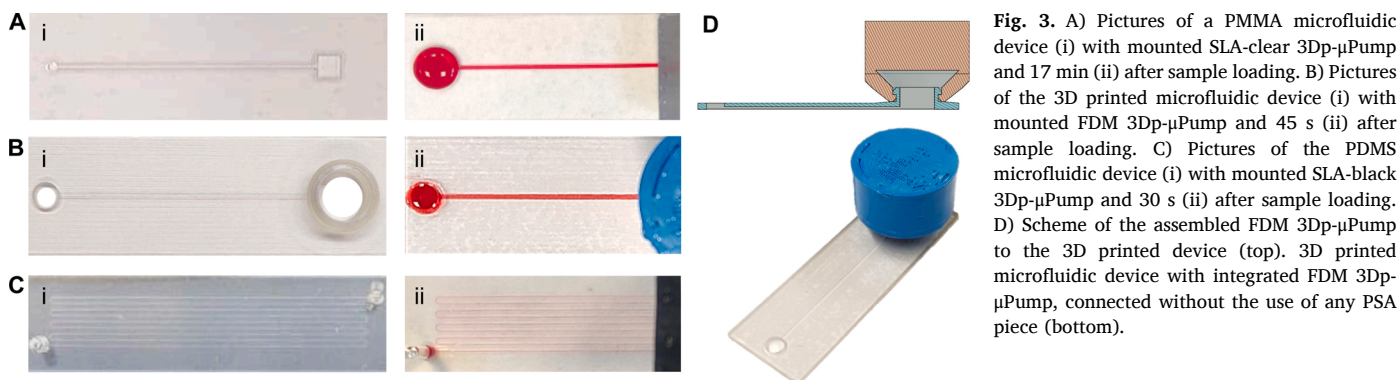
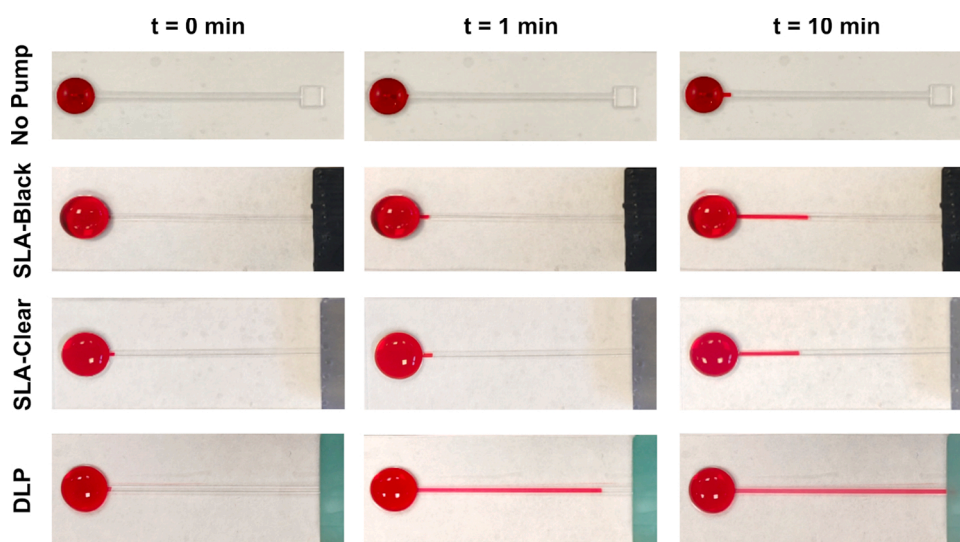


Fig. 2. Bottom and side view pictures of the 3Dp- $\mu$ Pumps manufactured by different technologies and materials: A) SLA-FLFLGR02 (SLA-black); B) SLA-FLFLGR01 (SLA-clear); C) DLP and (D) FDM.



**Fig. 3.** A) Pictures of a PMMA microfluidic device (i) with mounted SLA-clear 3Dp- $\mu$ Pump and 17 min (ii) after sample loading. B) Pictures of the 3D printed microfluidic device (i) with mounted FDM 3Dp- $\mu$ Pump and 45 s (ii) after sample loading. C) Pictures of the PDMS microfluidic device (i) with mounted SLA-black 3Dp- $\mu$ Pump and 30 s (ii) after sample loading. D) Scheme of the assembled FDM 3Dp- $\mu$ Pump to the 3D printed device (top). 3D printed microfluidic device with integrated FDM 3Dp- $\mu$ Pump, connected without the use of any PSA piece (bottom).



**Fig. 4.** Pictures of a multilayer PMMA thermo-laminated device (380  $\mu$ m height, 1 mm width and 50 mm length) without 3Dp- $\mu$ Pump, connected to a SLA-black, SLA-clear and DLP 3Dp- $\mu$ Pumps at times 0, 1 and 10 min, after loading of the sample.

### 3.2. 3Dp- $\mu$ Pumps versatility

Previous publications have shown that the flow rate of the vacuum pump depends on the properties of the material and on the effective suction surface, that is, the surface of the micropump that absorbs the air. And, on the other hand, it has also been seen that polymeric micropumps lose suction capacity over time as they fill with air [11,13,18]. To evaluate the effect of the polymer surface exposed to the microchannel on the pressure exerted by 3Dp- $\mu$ Pumps, the flow rate generated by different micropumps of increasing surface area was characterised. Micropumps of multiple SLA-black printed units (x1 to x4 units) were fabricated (see experimental methods for details) and mounted on PMMA thermo-laminated microfluidic chips (380  $\mu$ m height, 1 mm wide and 50 mm long). Subsequently, the flow rate produced by each pump was characterised by the digital microscope to monitor the liquid front motion inside the microchannel. Average flow rates of 0.25  $\mu$ L  $\text{min}^{-1}$ , 1.50  $\mu$ L  $\text{min}^{-1}$ , 2.00  $\mu$ L  $\text{min}^{-1}$  and 2.50  $\mu$ L  $\text{min}^{-1}$  were measured for the x1, x2, x3 and x4 units micropumps. In all cases, maximum flow rates were achieved during the first minutes, followed by an exponential decrease. After 2 min, the flow rate showed a more stable regime which lasted for about an hour. The micropumps slowly recovered the air, previously evacuated by degas and, therefore, their suction capacity decreased with time until reaching the equilibrium and stopping the flow. The generated flow rates were proportional to the number of units of each SLA-black 3Dp- $\mu$ Pump (see Fig. 5). Among the different SLA 3Dp- $\mu$ Pumps, a lower decrease in the flow rate was observed when

the number of units was low (x1 > x2 > x3 > x4).

Additionally, in order to confirm that the liquid did not move through the channel unless a micropump was adhered to the outlet of the device, the same characterisation was performed but without any micropump. 90  $\mu$ L of red dyed water were added to the inlet of the PMMA microchannel, no movement of the liquid inside the channel was appreciated after 10 min observation, see Video 6. This experiment indicated that only the negative pressure provided by the micropump could trigger the movement of the liquid.

The behaviour of the 3Dp- $\mu$ Pumps was similar to that of other polymeric micropumps [11,18]. Nevertheless, their flow rate was lower than PDMS micropumps of similar configurations [18], indicating lower air solubility in the SLA-black resin than in the PDMS. In conclusion, these results evidenced that the suction force is adjustable, depending on the 3Dp- $\mu$ Pump surface area exposed to the microchannel, since the flow rates increased with the number of units, 3Dp- $\mu$ Pump (xN), in the same way as in the previously published PDMS micropumps [18].

### 3.3. Autonomous colorimetric test for starch detection

As an example of a self-powered colorimetric test, enabled by the 3Dp- $\mu$ Pumps combined with a plastic microfluidic cartridge, we demonstrated the performance of an autonomous device for the detection of starch by the lugol-starch reaction. For this purpose, a 3Dp- $\mu$ Pump was attached to a multi-layered microfluidic device. The microchannel configuration was a single channel with a circular trench

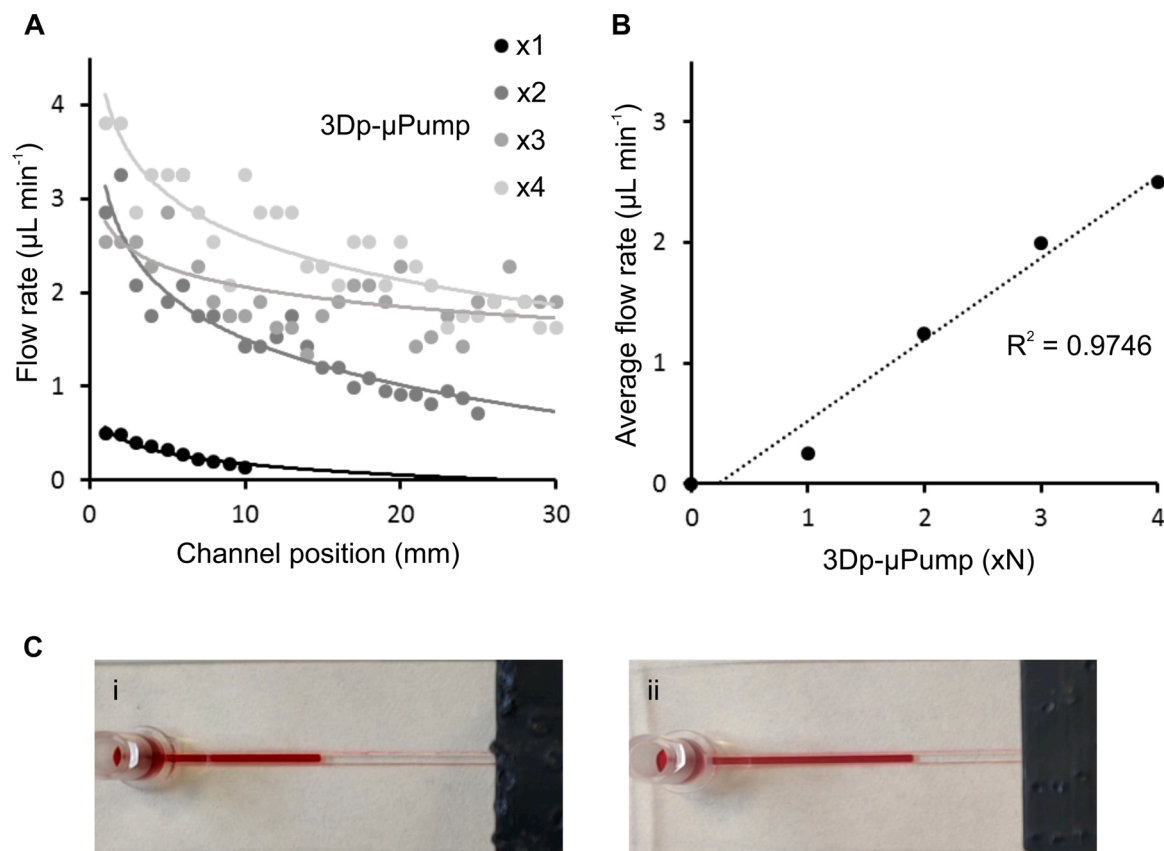


**Fig. 5.** A) SLA-black 3Dp- $\mu$ Pumps flow rates characterisation using increasing number of units (1, 2, 3 and 4). B) Linear regression of the average flow rate of the SLA-black 3Dp- $\mu$ Pumps using increasing number of units. C) Pictures of two PMMA microfluidic device (380  $\mu\text{m}$  height, 1 mm width and 50 mm length) with integrated SLA-black 3Dp- $\mu$ Pump of 3 units (i) and 4 units (ii) at 4 min.

where the transparent starch gel was placed. During the starch determination, a change of colour should be observed when the lugol solution reaches the trench and touches the starch gel, turning it into an intense "blue-black" colour. This reaction is widely named as the iodine-test and it is often used for starch determination in food samples [44]. A x4-units SLA-black 3Dp- $\mu$ Pump was mounted on the outlet of the plastic cartridge and 100  $\mu\text{L}$  of lugol solution was loaded into the inlet. The lugol sample slowly filled the trench and, after several minutes, all the gelled starch acquired a bluish-black colour. Finally, the lugol solution continued flowing through the microchannel towards the SLA 3Dp- $\mu$ Pump reservoir (see Fig. 6 and Video 7). The microfluidic device was able to

autonomously work, despite the high flow resistance and the large volume of the device, demonstrating the possibility of generating functional integrated self-powered analytical microdevices with 3Dp- $\mu$ Pumps and plastic microfluidic cartridges.

#### 4. Conclusions

Rapid point-of-care analysis is one of the most important applications of microfluidics. To facilitate the implementation of this technology, there is a great demand for microfluidic architectures that do not require electronic instrumentation to control the flow of samples within

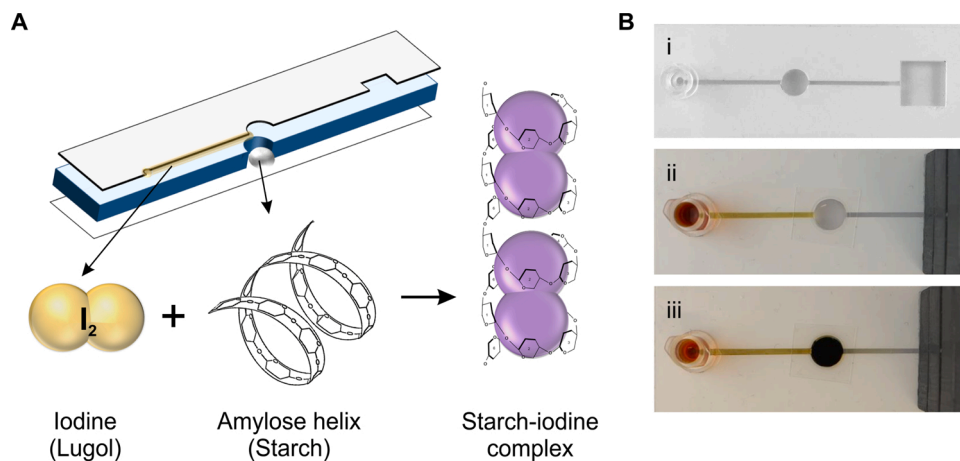


**Fig. 6.** A) Scheme of the iodine-starch reaction inside of the microfluidic device. B) Pictures of the layer-by-layer microfluidic device for starch detection (i) at time 1 min (ii) and 18 min (iii) after loading the lugol solution (yellow). The 4-units SLA-black 3Dp- $\mu$ Pump was responsible for the autonomous operation of the device.

the microchannels. During the last 8 years, it has been demonstrated the possibility of manufacturing modular polymeric micropumps with the idea of having modular architectures: microfluidic cartridges and micropumps, which can be assembled to generate self-powered devices. The idea is very attractive as a universal architecture for POC analysis devices, but, in order to get to that point, it is necessary to have a versatile manufacturing technique that would enable the easy fabrication of customised micropumps and cartridge designs.

In this work, we demonstrated that 3D printing is a highly versatile technique for the fabrication of modular polymeric micropumps to create autonomous flow microsystems. As a proof of concept, we demonstrated the development of an autonomous colorimetric test for starch detection. Different manufacturing techniques using 3D printing allowed the fabrication of parts with polymeric materials, quickly and easily. The micropumps can be assembled with diverse microfluidic devices manufactured by different methods, material composition (resins) and dimensions. It was demonstrated that the negative pressure provided by the micropumps is responsible for the movement of the liquid through the microchannels. In addition, the flow rate generated by the micropumps is tuneable because the pressure provided by the micropumps depends on the suction characteristics of the material and their air absorption surface. Since there are a wide variety of 3D printing methods and the range of designs and materials that can be used is huge, this strategy enables the manufacturing of customised micropumps according to the needs of the application. Last but not least, for the first time, we showed an alternative to create geometries that cannot be manufactured with normal fabrication techniques, by presenting an improved strategy for direct assembly of micropumps and microfluidic cartridges, demonstrating a truly universal methodology. For all stated above, 3D manufactured micropumps arise as an innovative element in the field of self-powered microfluidics, which could become a key element for the development of integrated microsystems for applications such as rapid analysis at the point-of-care.

#### CRedit authorship contribution statement

**Y. Alvarez-Braña:** Methodology, Validation, Investigation, Data curation, Writing - original draft, Writing - review & editing, Visualization. **J. Etxebarria-Elezgarai:** Methodology, Data curation, Formal analysis, Writing - original draft. **L. Ruiz de Larrinaga-Vicente:** Investigation. **F. Benito-Lopez:** Resources, Writing - original draft, Writing - review & editing, Visualization, Supervision, Project administration, Funding acquisition. **L. Basabe-Desmots:** Conceptualization, Formal analysis, Funding acquisition, Methodology, Supervision, Writing - original draft, Writing - review & editing.

#### Declaration of Competing Interest

The authors declare that they have no known competing financial interests or personal relationships that could have appeared to influence the work reported in this paper.

#### Acknowledgements

Authors would like to acknowledge the funding support from Gobierno de España, Ministerio de Economía y Competitividad, with Grant No. BIO2016-80417-P (AEI/FEDER, UE); the University of the Basque Country (ESPPOC 16/65) and Gobierno Vasco Dpto. Educación for the consolidation of the research groups (IT1271-19). FBL acknowledges the Ramón y Cajal programme (Ministerio de Economía y Competitividad). FBL and LBD acknowledge the “Red de Microfluidica Española” MIFLUNET (RED2018-102829-T). Authors acknowledge to Prof. Javier del Campo and to Dr. Cristian Mendes from BC Materials, Spain, for their help during the fabrication of the micropumps with the DLP technique.

#### Appendix A. Supplementary data

Supplementary material related to this article can be found, in the online version, at doi:<https://doi.org/10.1016/j.snb.2021.129991>.

#### References

- [1] K. Iwai, K.C. Shih, X. Lin, T.A. Brubaker, R.D. Sochol, L. Lin, Finger-powered microfluidic systems using multilayer soft lithography and injection molding processes, *Lab Chip* 14 (2014) 3790–3799.
- [2] M.T. Guler, Z. Isiksacan, M. Serhatlioglu, C. Elbuken, Self-powered disposable prothrombin time measurement device with an integrated effervescent pump, *Sens. Actuators B Chem.* 273 (2018) 350–357.
- [3] Y. Temiz, E. Delamarche, Capillary-driven microfluidic chips for miniaturized immunoassays: efficient fabrication and sealing of chips using a “Chip-Olate” process, *Methods Mol. Biol.* 1547 (2017) 25–36.
- [4] T. Kokalj, Y. Park, M. Vencelj, M. Jenko, L.P. Lee, Self-powered imbibing microfluidic pump by liquid encapsulation: SIMPLE, *Lab Chip* 14 (2014) 4329–4333.
- [5] X. Li, J. Tian, W. Shen, Thread as a Versatile Material for Low-Cost Microfluidic Diagnostics, *ACS Appl. Mater. Interfaces* 2 (2010) 1–6.
- [6] M.M. Erenas, I. de Orbe-Payá, L.F. Capitan-Vallvey, Surface modified thread-based microfluidic analytical device for selective potassium analysis, *Anal. Chem.* 88 (2016) 5331–5337.
- [7] L. Dong, H. Jiang, Autonomous microfluidics with stimuli-responsive hydrogels, *Soft Matter* 3 (2007) 1223–1230.
- [8] J. ter Schiphorst, J. Saez, D. Diamond, F. Benito-Lopez, A.P.H.J. Schenning, Light-responsive polymers for microfluidic applications, *Lab Chip* 18 (2018) 699–709.
- [9] T. Akyazi, A. Tudor, D. Diamond, L. Basabe-Desmots, L. Florea, F. Benito-Lopez, Driving flows in microfluidic paper-based analytical devices with a cholinium based poly(ionic liquid) hydrogel, *Sens. Actuators B Chem.* 261 (2018) 372–378.
- [10] E. Yeh, C. Fu, L. Hu, R. Thakur, J. Feng, L.P. Lee, Self-powered integrated microfluidic point-of-care low-cost enabling (SIMPLE) chip, *Sci. Adv.* 3 (2017), e1501645.
- [11] G. Li, Y. Luo, Q. Chen, L. Liao, J. Zhao, A “place n play” modular pump for portable microfluidic applications, *Biomicrofluidics* 6 (2012), 014118.
- [12] D.Y. Liang, A.M. Tentori, I.K. Dimov, L.P. Lee, Systematic characterization of degas-driven flow for poly(dimethylsiloxane) microfluidic devices, *Biomicrofluidics* 5 (2011) 24108.
- [13] K. Hosokawa, M. Omata, K. Sato, M. Maeda, Power-free sequential injection for microchip immunoassay toward point-of-care testing, *Lab Chip* 6 (2006) 236–241.
- [14] I.K. Dimov, L. Basabe-Desmots, J.L. Garcia-Cordero, B.M. Ross, A.J. Ricco, L. P. Lee, Stand-alone self-powered integrated microfluidic blood analysis system (SIMBAS), *Lab Chip* 11 (2011) 845–850.
- [15] Y. Fu, H. Zhou, C. Jia, F. Jing, Q. Jin, J. Zhao, G. Li, A microfluidic chip based on surfactant-doped polydimethylsiloxane (PDMS) in a sandwich configuration for low-cost and robust digital PCR, *Sens. Actuators B Chem.* 245 (2017) 414–422.
- [16] K. Hosokawa, K. Sato, N. Ichikawa, M. Maeda, Power-free poly(dimethylsiloxane) microfluidic devices for gold nanoparticle-based DNA analysis, *Lab Chip* 4 (2004) 181–185.
- [17] K. Hasegawa, M. Matsumoto, K. Hosokawa, M. Maeda, Detection of methylated DNA on a power-free microfluidic chip with laminar flow-assisted dendritic amplification, *Anal. Sci.* 32 (2016) 603–606.
- [18] J. Etxebarria-Elezgarai, Y. Alvarez-Braña, R. Garoz-Sanchez, F. Benito-Lopez, L. Basabe-Desmots, Large-volume self-powered disposable microfluidics by the integration of modular polymer micropumps with plastic microfluidic cartridges, *Ind. Eng. Chem. Res.* 59 (2020) 22485–22491.
- [19] G. Weisgrab, A. Ovsianikov, P.F. Costa, Functional 3D printing for microfluidic chips, *Int. J. Adv. Mater. Technol.* 4 (2019), 1900275.
- [20] E. MacDonald, R. Wicker, Multiprocess 3D printing for increasing component functionality, *Science* 353 (2016), aaf2093.
- [21] A.K. Au, W. Huynh, L.F. Horowitz, A. Folch, 3D-Printed microfluidics, *Angew. Chem. Int. Ed.* 55 (2016) 3862–3881.
- [22] B. Gross, S.Y. Lockwood, D.M. Spence, Recent advances in analytical chemistry by 3D printing, *Anal. Chem.* 89 (2017) 57–70.
- [23] A. Arivarasi, A. Kumar, Classification of challenges in 3D printing for combined electrochemical and microfluidic applications: a review, *Rapid Prototyp. J.* 25 (2019) 1328–1346.
- [24] S. Mi, Z. Du, Y. Xu, W. Sun, The crossing and integration between microfluidic technology and 3D printing for organ-on-chips, *J. Mater. Chem. B Mater. Biol. Med.* 6 (2018) 6191–6206.
- [25] J. Wang, C. McMullen, P. Yao, N. Jiao, M. Kim, J. Kim, L. Liu, S. Tung, 3D-printed peristaltic microfluidic systems fabricated from thermoplastic elastomer, *Microfluid. Nanofluidics* 21 (2017) 105.
- [26] Z. Jiao, L. Zhao, C. Tang, H. Shi, F. Wang, B. Hu, Droplet-based PCR in a 3D-printed microfluidic chip for miRNA-21 detection, *Anal. Methods* 11 (2019) 3286–3293.
- [27] H. Hong, J.M. Song, E. Yeom, 3D printed microfluidic viscometer based on the flowing stream, *Biomicrofluidics* 13 (2019), 014104.
- [28] E.K. Parker, A.V. Nielsen, M.J. Beauchamp, H.M. Almughamsi, J.B. Nielsen, M. Sonker, H. Gong, G.P. Nordin, A.T. Woolley, 3D printed microfluidic devices with immunoaffinity monoliths for extraction of preterm birth biomarkers, *Anal. Bioanal. Chem.* 411 (2019) 5405–5413.

- [29] J. Nie, Q. Gao, J. Qiu, M. Sun, A. Liu, L. Shao, J. Fu, P. Zhao, Y. He, 3D printed Lego®-like modular microfluidic devices based on capillary driving, *Biofabrication* 10 (2018), 035001.
- [30] G. Weisgrab, A. Ovsianikov, P.F. Costa, Functional 3D printing for microfluidic chips, *Int. J. Adv. Mater. Technol.* 4 (2019), 1900275.
- [31] H. Gong, A.T. Woolley, G.P. Nordin, High density 3D printed microfluidic valves, pumps, and multiplexers, *Lab Chip* 16 (2016) 2450–2458.
- [32] A.K. Au, N. Bhattacharjee, L.F. Horowitz, T.C. Chang, A. Folch, 3D-printed microfluidic automation, *Lab Chip* 15 (2015) 1934–1941.
- [33] J. Wang, C. McMullen, P. Yao, N. Jiao, M. Kim, J.W. Kim, L. Liu, S. Tung, 3D-printed peristaltic microfluidic systems fabricated from thermoplastic elastomer, *Microfluid. Nanofluid.* 21 (2017) 105.
- [34] M.N.H.Z. Alam, F. Hossain, A. Vale, A. Kouzani, Design and fabrication of a 3D printed miniature pump for integrated microfluidic applications, *Int. J. Precis. Eng. Manuf. Technol.* 18 (2017) 1287–1296.
- [35] M.R. Behrens, H.C. Fuller, E.R. Swist, J. Wu, M.M. Islam, Z. Long, W.C. Ruder, R. Steward, Open-source, 3D-printed peristaltic pumps for small volume point-of-Care liquid handling, *Sci. Rep.* 10 (2020) 1543.
- [36] M.B. Habbab, T. Ismail, J.F. Lo, A laminar flow-based microfluidic tesla pump via lithography enabled 3D printing, *Sensors*. 16 (2016) 1970.
- [37] E.C. Sweet, R.R. Mehta, R. Lin, L. Lin, Finger-powered, 3D printed microfluidic pumps, in: 19th International Conference on Solid-State Sensors, Actuators and Microsystems (TRANSDUCERS), Kaohsiung, Taiwan, 2017, pp. 1766–1769.
- [38] Z. Tang, X. Shao, J. Huang, G. Ding, J. Yao, 3D printed pump based on vibrating blades to actively manipulate fluid, *IOP Conf. Ser.: Earth Environ. Sci.* 267 (2019), 042168.
- [39] A.P. Taylor, L.F. Velásquez-García, Low-cost, monolithically 3D-printed, miniature high-flow rate liquid pump, *J. Phys. Conf. Ser.* 1407 (2019), 012040.
- [40] D.J. Thomas, Z. Tehrani, B. Redfeare, 3-D printed composite microfluidic pump for wearable biomedical applications, *Addit. Manuf.* 9 (2016) 30–38.
- [41] N.N. Cuong, L.V. Luan, N.N. An, T.D. Van, T.B. Tung, C.D. Trinh, A valveless micropump based on additive fabrication technology, *Int. J. Nanotechnol.* 15 (2018) 11–12.
- [42] H.N. Chan, Y. Shu, B. Xiong, Y. Chen, Y. Chen, Q. Tian, S.A. Michael, B. Shen, H. Wu, Simple, cost-effective 3D printed microfluidic components for disposable, point-of-care colorimetric analysis, *ACS Sens.* 1 (2016) 227–234.
- [43] M. Garcia-Hernando, A. Calatayud-Sanchez, J. Etxebarria-Elezgarai, M.M. de Pancorbo, F. Benito-Lopez, L. Basabe-Desmots, Optical single cell resolution cytotoxicity biosensor based on single cell adhesion dot arrays, *Anal. Chem.* 92 (2020) 9658–9665.
- [44] M. Pospiech, M. Petrášová, B. Tremlová, Z. Randulová, Detection of native starches in meat products using histochemical Lugol Calleja method, *Potravinárstvo* 8 (2014) 77–81.

**Yara Alvarez Braña** studied Biotechnology at Oviedo University. In 2017, she finished her Master Degree in Forensic Analysis, which allowed her to begin her research career in the group Microfluidics Cluster UPV/EHU, at the University of the Basque Country. Currently she is a PhD student in the Materials Science and Technology Program at the Microfluidic Cluster UPV/EHU working on the modular development, fabrication and integration of autonomous microfluidics devices and its applications.

**Jaione Etxebarria Elezgarai** has a M.Sc. in Chemical Engineering (2008) and a post-graduate master in Engineering of advanced materials (2010) from the University of the Basque Country in Bilbao. In 2015 she completed her doctoral thesis in polymeric microsystems for flow control and sensing applications in Lab-on-a-chip (LOC) systems at the Microsystems department of IK4-Ikerlan Research Center. Then, she continued her postdoctoral research in the Microfluidics Cluster UPV/EHU, at the University of the Basque Country for three years, and currently she is working in the nanoengineering group at CIC-nanoGUNE as a postdoctoral research associate to establish novel biosensing tools for liquid biopsy based on plasmonic sensing. In particular, her activities are focused in generating multidisciplinary biomedical microsystems that cover areas such as material science, micro/nano manufacturing technologies, microfluidics, integration of fluidic/mechanical/optical/electronic components in microsystems for LOC and Point-of-Care (POC) rapid analysis devices, adaptation and validation of biological laboratory protocols into LOC and POC systems, and optimization of their respective detection techniques.

**Lorena Ruiz de Larrinaga** studied Biotechnology at the Basque Country University (UPV/EHU). During two years she has been working at Plant Biology and Ecology laboratories (UPV/EHU) where she developed knowledge in High Pressure Liquid Chromatography (HPLC), phytochemicals and circadian rhythms in postharvest vegetables. In 2019, she finished her second degree in Biochemistry at UPV/EHU and developed her final degree project at the Microfluidic Cluster UPV/EHU group, which deals with the development of point of care diagnostic test for rapid blood analysis.

**Fernando Benito-Lopez** studied chemistry at the Universidad Autonoma de Madrid and completed his master studies in the Departments of Inorganic and Analytical Chemistry in 2002. He obtained his PhD at the University of Twente, The Netherlands, in 2007. He carried out his postdoctoral research in the group of Prof. Dermot Diamond at Dublin City University, Dublin, where in 2010, he became Team Leader in polymer microfluidics. In 2012 he moved to CIC microGUNE a Research Centre working in Microtechnology in Spain. In 2015 he was awarded with the Ramón y Cajal Fellow and became leader of the Analytical Microsystems & Materials for Lab-on-a-Chip (AMMA-LOAC) Group, Microfluidics Cluster UPV/EHU, at the University of the Basque Country, Spain. From July 2019 he is Assoc. Prof. at the same university.

**Lourdes Basabe-Desmots** is an IKERBASQUE Research Professor and the group leader of BIOMICS microfluidics Research Group at the University of the Basque Country (UPV/EHU). Her team is focused on the development of microtechnologies for lab-on-a-chip applications for biology and medicine, comprising areas such as chemistry, micro and nano engineering of surfaces, optical sensing, microfluidics, microsystems for single cell studies and point of care diagnostics. She is co-founder of the Microfluidics Cluster UPV/EHU. Lourdes studied Chemistry at the Universidad Autonoma de Madrid, then she did a PhD at the University of Twente in Supramolecular Chemistry and Nanotechnology. Following she joined the Biomedical Diagnostics Institute in Dublin where after a postdoc in polymer microfluidics she became a team leader on “microtechnologies for platelet biology”. In June 2012 she was appointed Research Professor by IKERBASQUE the Basque Foundation of Science in Spain.